Experimental Study of Electrical Break Down and Onset of Combustion of Inductive and Capacitive Sparks for Ignition Systems

Diploma paper by
Jonas G. Bengtsson and Lars Nilsson

LRAP-78
Dept. of Physics, Lund Institute of technology,
P.O. Box 725, S-220 07 Lund, Sweden, together
with Mecel AB of SAAB-Scania-Combitech,
Box 32, S-662 00 Åmål, Sweden.

Lund Reports on Atomic Physics

LRAP-78

September 1987

CONTENTS

1. Abstract.

The purpose of this study is to get a survey of the influence of different parameters on spark generation and flame speed in a burning gas. Statistical time lags and breakdown voltage distributions were measured and three different electrical systems for spark generation were used (two commercial systems and one specially designed with very fast voltage ramp rate). Different electrode materials, effects of pressure and surrounding gas were studied. The flame speed measurements were made using the two commercial ignition systems with steel and copper electrodes and made for different air-methane mixtures.

2.1.1. Introduction to statistical time-lag measurements

When a voltage ramp is applied on a spark gap the gap will eventually break down at a certain voltage. The characteristics of the probability density functions for the delay times are recorded. Its characteristics will depend on different parameters. Naturally the voltage ramp rate and the current provided by the electrical circuit is important. The probability density function will also depend on the choice of electrodes, the width of the spark gap and the surrounding gas.

The initial stages of sparks depend critically on the initial number density of free charges in the gas and on the condition of the electrode surfaces.
A mathematical model for predicting the characteristics of the voltage distribution has been proposed by for instance Gordon et al[1]. The model predicts that increasing the pressure or the voltage charging both produce a broadening of the voltage distribution.

It is important how the electrode's surface conditions are continuously changed due to wear and chemical reactions with the surrounding gas. The surface conditions can have large effects on the probability distribution. A study where the surfaces of the electrodes have been examined have been made by for instance Gordon et al[2].
The fact that the electrode surfaces are continuosly changing makes it difficult to obtain reproducible experiments.
We have chosen to study breakdown voltage probability density functions for some different materials with different gases at different pressures. The voltage distributions presented here are based on 150-200 sparks.

Three different electrical circuits have been used to provide voltage ramps. One arrangement was used for the production of very fast voltage ramps, described in section 2.2.1, and two different commercial systems, one capacitive ignition system (see 2.3.1) with a faster voltage ramp than the third, a conventional inductive ignition system by Bosch (see 2.4.1). The energy transferred for the different electrical circuits are shown in fig. 2.1.1.

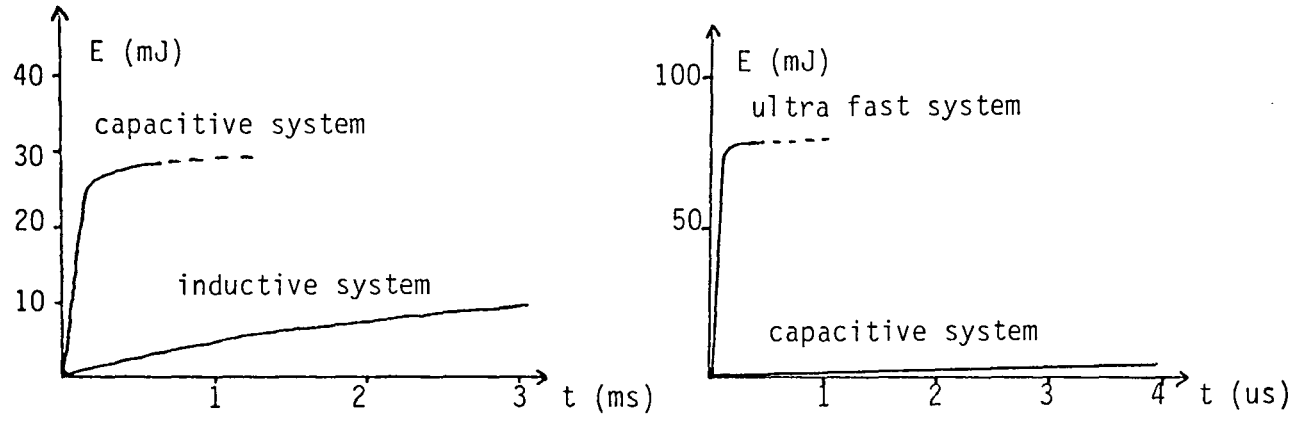

Fig.2.1.1: Energy transferred for different electrical circuits.

The probability density function for the delay times to breakdown has been measured and the probability for breakdown has been calculated.

The purpose of our study has been to get a survey on how different choice of electrode materials and gas influence on the breakdown voltage distribution. We also wanted to compare two commercially available ignition systems.

2.1.2 Waiting times for breakdown, theory.

A fall in the applied voltage over the spark gap indicates the start of break down. If the voltage is applied at a time t_o there will be a waiting time θ before the breakdown occurs. The time θ from t_o is a random variable with values in the range $(0,\infty)$ and the quantity of interest is its probability density $w(\theta,t_o)$. $w(\theta,t_o)$ depends parametrically on t_o unless the random sets of

events are stationary. Later we will give experimentally recorded $w(\theta,t_o)$.

We will now express $w(\theta,t_o)$ in terms of quantities that specify the random set. Let $p_o(t_o,t_o+\theta)$ denote the probability that no breakdown occurs between t_o and $t_o+\theta$. Then the probability $w(\theta,t_o)\delta\theta$ that the first breakdown occurs between $t_o+\theta$ and $t_o+\theta+\delta\theta$ is $p_o(t_o,t_o+\theta)-p_o(t_o,t_o+\theta+\delta\theta)$. This gives:

$$w(\theta,t_o) = -(\delta/\delta\theta)p_o(t_o,t_o+\theta)$$

and also

$$p_o(t_o,t_o+\theta) = 1 - \int_0^\theta w(\theta,t_o)\delta\theta$$

$p_o(t_o,t_o+\theta)$ may be expressed in distribution or correlation functions and accordingly $w(\theta,t_o)$. The applied voltage is a function of time and may be used as a variable in the probability functions after well known transformations have been done. This representation has also been used below. The development in correlation functions, distributions and relevant interpretations will be published elsewhere.

2.2.1 Experimental arrangement for ultra-short discharge

A discharge circuit was made according to fig. 2.2.1.

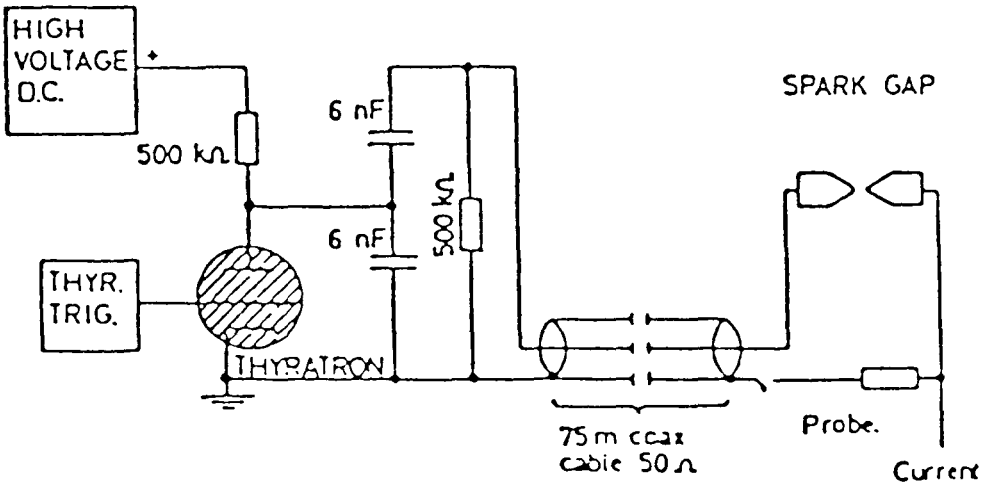

Fig. 2.2.1 : Electrical arrangement for spark generation.

When a trig pulse reaches the thyratron the charge on the lower capacitor will be discharged through the thyratron, causing a voltage reversal on the lower capacitor. Both capacitors will discharge through the 50 Ohm transmission line, creating a voltage ramp with typically 0.3 - 0.5 kV/ns in its linear region, see fig. 2.2.2. A long transmission line is used and reflected pulses will have no influence on our measurements.

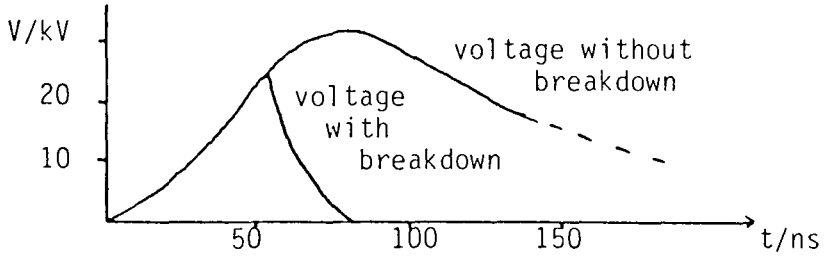

Fig. 2.2.2: Voltage ramp from fast system.

0.5 mm in a container that could be sealed and to which pressure be applied. At 1 MPa nitrogen was flowed vertically, perpendicular to the electrodes.

2.2.2 Results for ultra-short discharges.

The breakdown voltage was recorded on an oscilloscope screen. The approximate error of 20 percent was mainly due to difficulties in maintaining a constant gap length when pressure was applied. Since the voltage pulse could not be stored it was hard to obtain an accurate readout of the breakdown voltage.

The voltage distributions for Gd and Al electrodes are shown in figs. 2.2.5a and 2.2.5b. We can see that the voltage distributions for Gd are wider than for Al at low pressures. The breakdown voltage, as expected, is shifted towards higher values at higher pressure. The behaviour of the steel electrodes, fig. 2.2.5c, at increasing pressure can be explained by the fact that the gap length has increased when pressure was applied.

The expected broadening of the voltage distribution at higher pressure, that was predicted by Gordon[1], does not show up here. The voltage applied rises to several times the static breakdown voltage due to the fast voltage ramp, 10^6 times faster than that of Gordon[1] (0.3 - 0.5 kV/ns versus 60 - 0.3 kV/μs). The method may therefore not be applicable to our measurments.

Since the history of the electrodes used was unknown and an analysis of the surfaces was not possible we could not determine how the surface conditions changed during the experiment. We shall

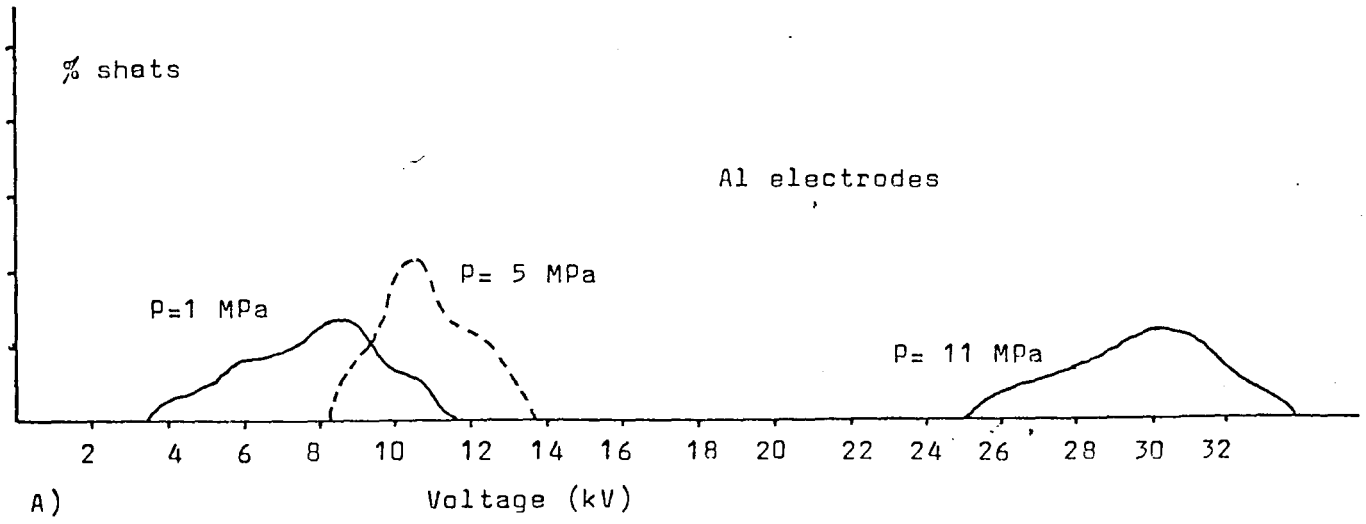

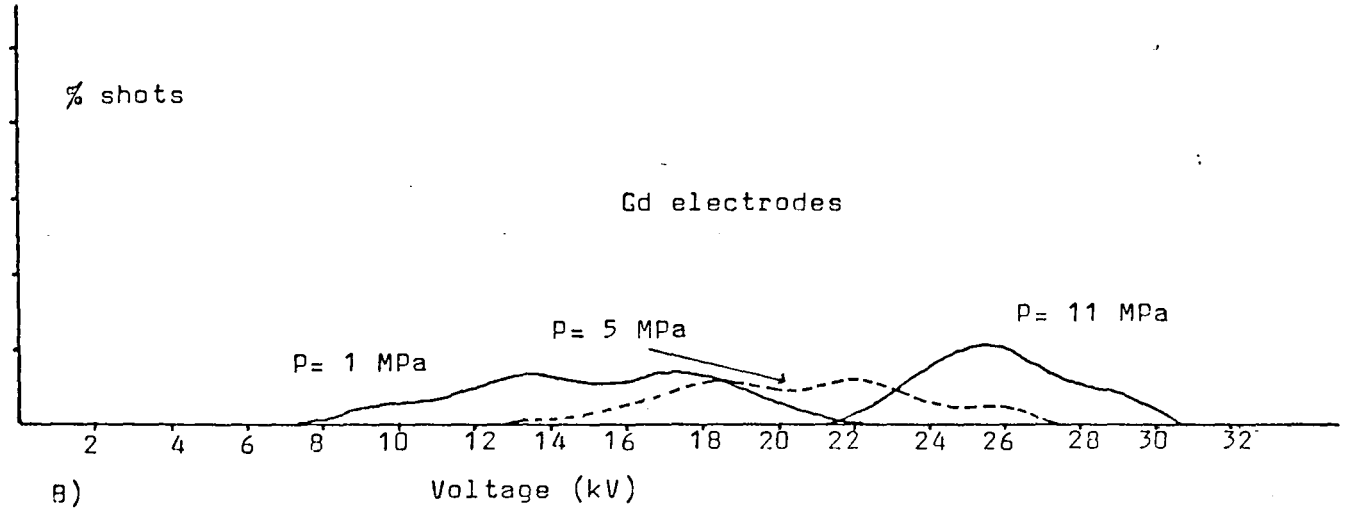

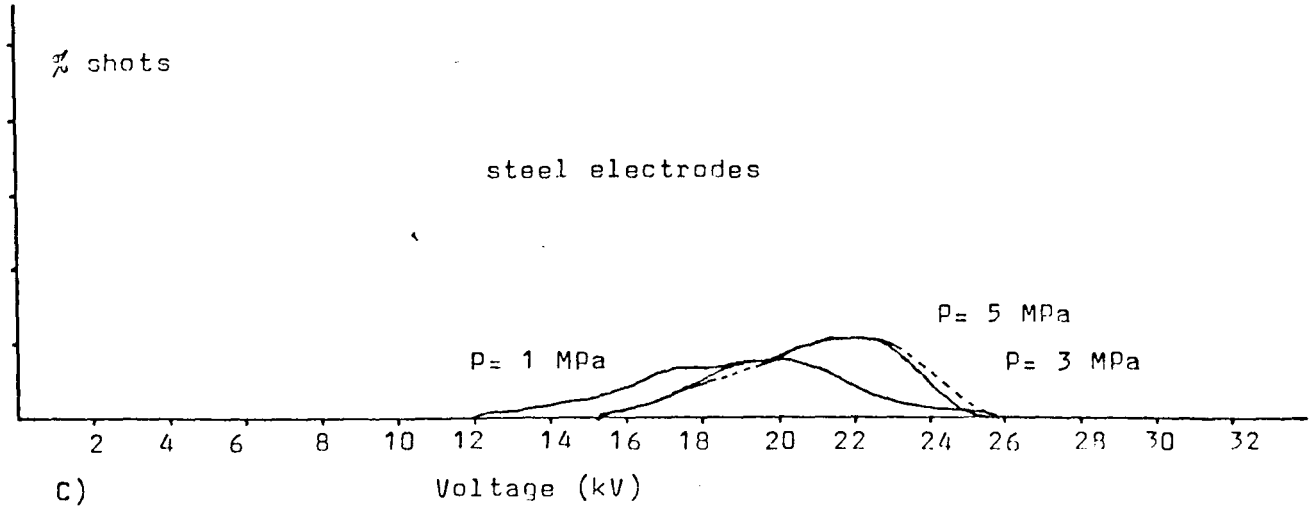

figs.2.2.5a-c Voltage distributions for different electrodes for ultra short discharge system.

discuss later how an oxide coating on the Al-electrodes probably changes their behaviour radically. The obtained voltage distributions should therefore be considered as qualitative.

Fig. 2.2.5b : Voltage distributions for gadolinium electrodes.
Fig. 2.2.5b : Voltage distributions for aluminium electrodes.
Fig. 2.2.5c : Voltage distributions for steel electrodes.

2.3.1 Experimental arrangement for capacitive discharge circuit

In the following experiment a discharge circuit based on a capacitiv discharge was used, fig. 2.3.1. The voltage ramp in the region of our measurements was typically 6kV/μs; see fig. 2.3.2, and the stored energy 30 mJ. The breakdown voltage was measured with a high-voltage probe and recorded on a digital memory oscilloscope. The error of our measurements was estimated to 10 percent.

Our measurments were made on a conventional sparking plug with steel electrodes. The electrodes were also changed to electrodes made of aluminium, gadolinium, copper and K33 (a tungsten-copper composite). Unfortunately, the sparking plugs were not made with the same spark gap lengths, except for the sparking plugs with Al and Gd electrodes. The spark gap lengths (d) were for Al d=0.6 mm ; Gd d=0.6 mm ; Steel d=0.85 mm ; K33 d=0.95 mm ; Cu d=1.1 mm. One sparking plug of another make with an Au/Pd cathode was also used (see 2.5.2).

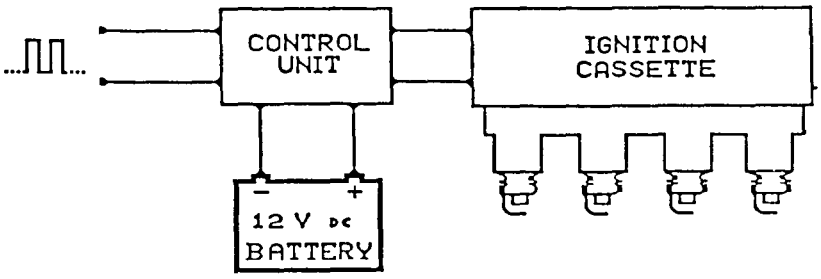

Fig. 2.3.1 : Experimental arrangement for capacitive discharge circuit.

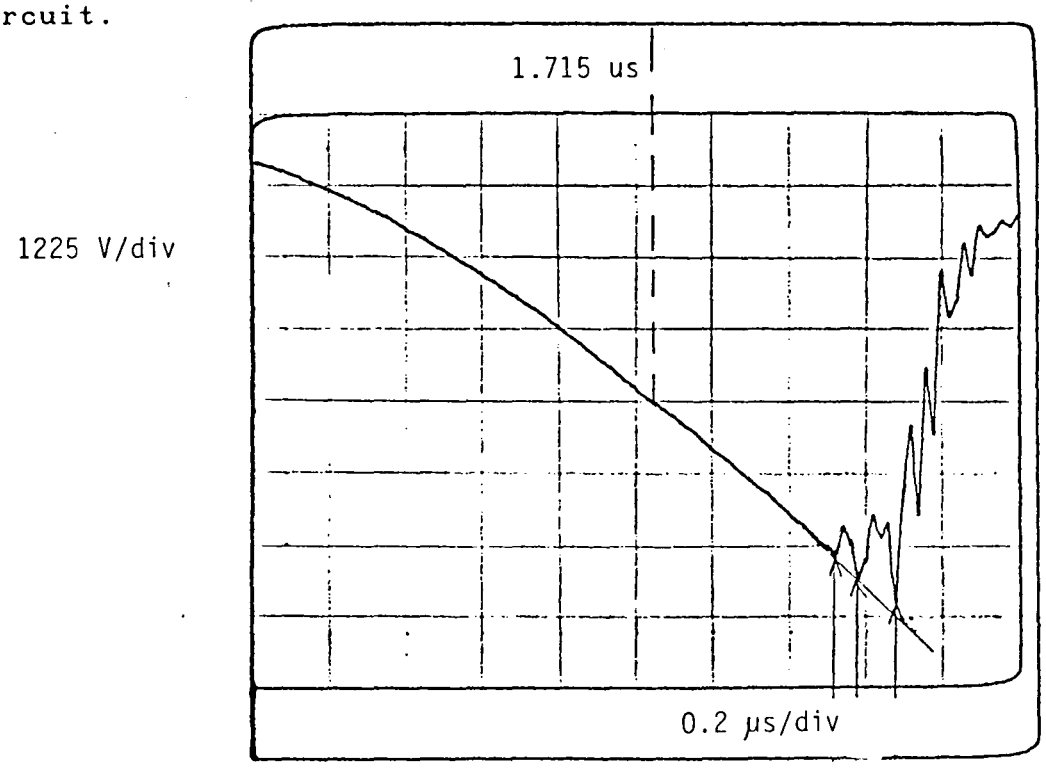

Fig. 2.3.2 : Voltage ramp for capacitive discharge circuit.

Measurements on the voltage distributions were made without any preceeding preparation of the electrodes, and when 6000 sparks at a rate of 10 Hz had been discharged directly before our measurements.The surrounding gas was nitrogen at a pressure of 1

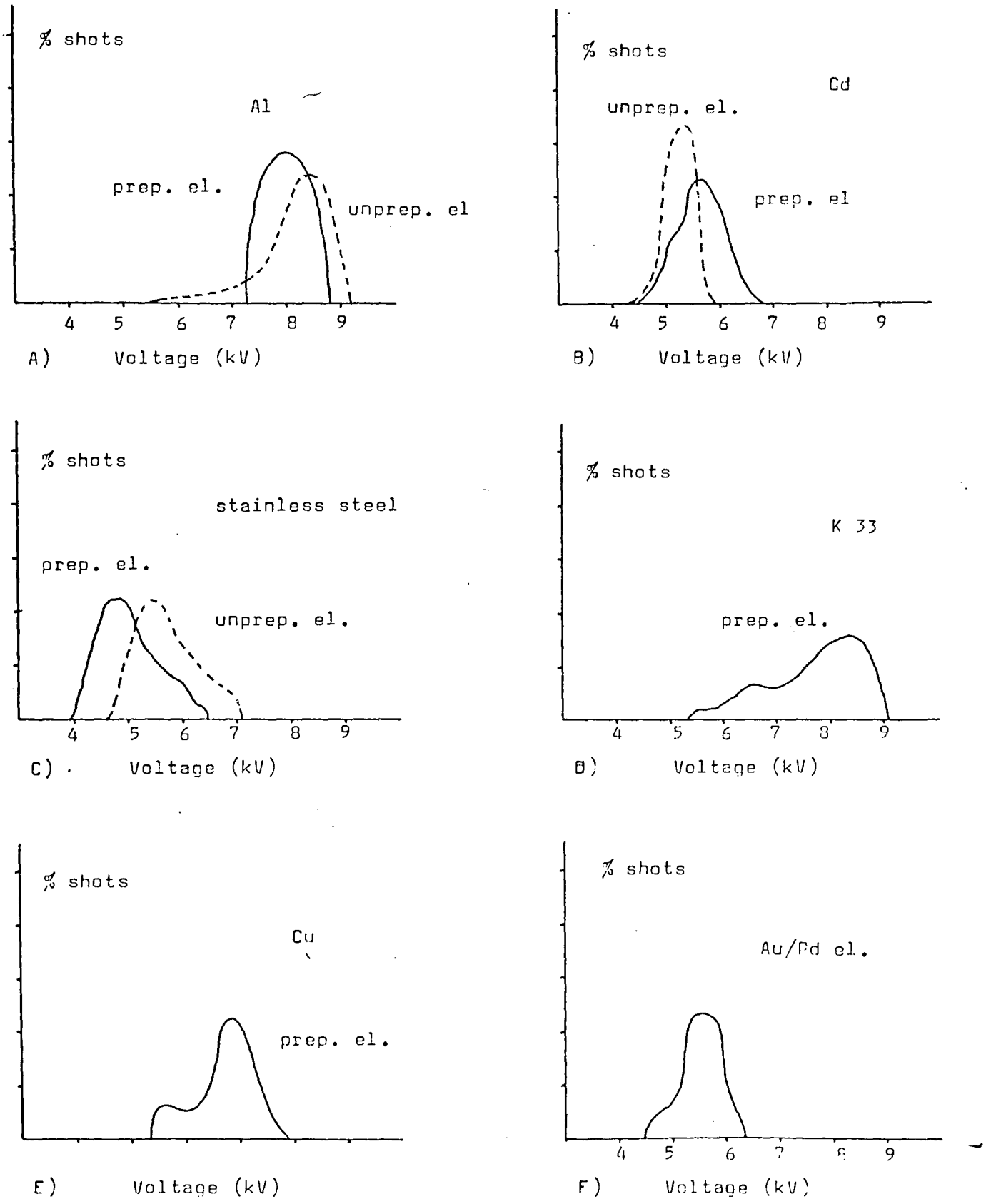

Figs. 2.3.3a-f Voltage distributions for different electrode materials for capacitive discharge system.

MPa. Our measurements on unprepared electrodes were recorded on an oscilloscope without storage possibilities and therefore with a higher estimated error of 20 percent.

2.3.2 Results for capacitive discharge circuit.

Voltage distributions are shown in figs. 2.3.3a-d. For aluminium electrodes we see that breakdown is possible at lower voltages when unprepared electrodes are used, compared to prepared ones. We also note that the breakdown voltage is lower for Gd than for Al and not the opposite as shown in our previous experiment. This, again shows how important the surface condition of the electrode is.

The differences in breakdown voltage for prepared and unprepared stainless steel electrodes lies within the limits of error. We note that the voltage distributions obtained with steel are similar to each other.

We see that the voltage distributions for K33 and copper both have two peaks.

2.4.1 Experimental arrangement for inductive discharge circuit

The third ignition system used, is a conventional system made by Bosch based on an inductively coupled discharge from a coil, see fig. 2.4.1. The voltage ramp, fig. 2.4.2 , is typically 300 V/µs and 20 times slower than that of the capacitive system. The energy transferred was approximately 10 mJ.

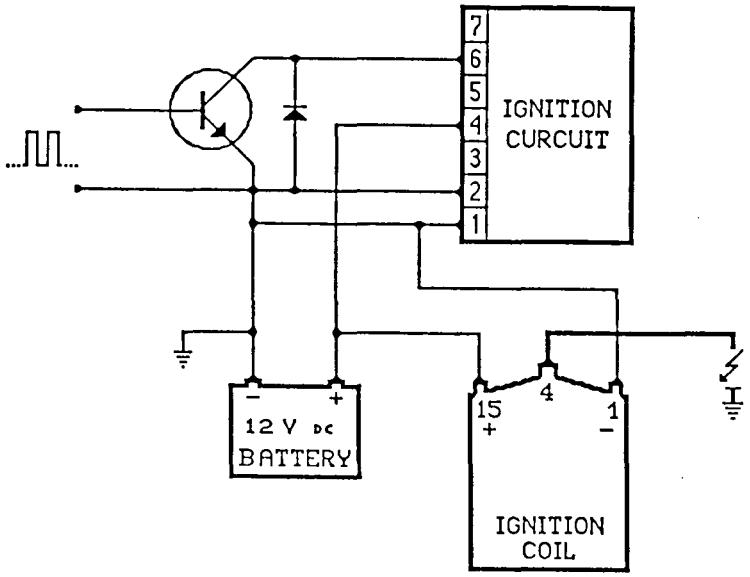

Fig. 2.4.1 : Inductive discharge circuit.

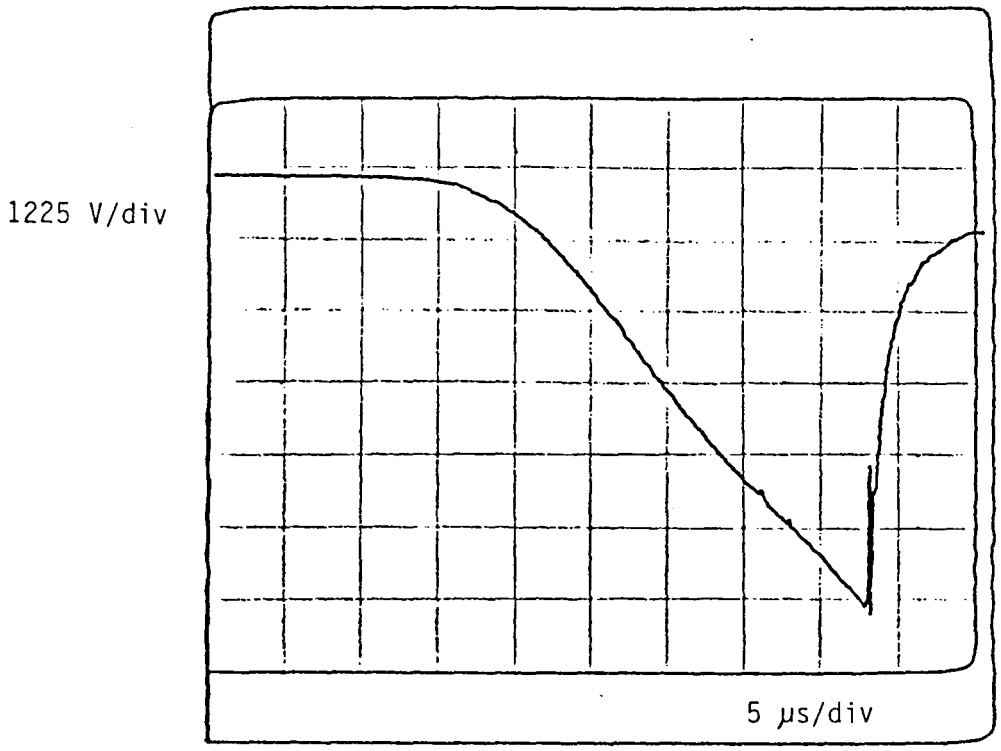

Fig. 2.4.2 : Voltage ramp for inductive discharge circuit.

The breakdown voltage was measured in the same way as before with a high voltage probe and recorded on a digital memory oscilloscope. When measurements were made on unprepared electrodes an oscilloscope without storage possibilities were used, and those measurements are therefore less accurate. The same sparking plugs as in the previous experiment were used. The surrounding gas was again nitrogen at 1 MPa.

2.4.2 Results for inductive discharge system and a comparison with the capacitive discharge system.

Voltage distributions are shown in figs. 2.4.3a-e. The breakdown voltage is considerably lower for unprepared Al-

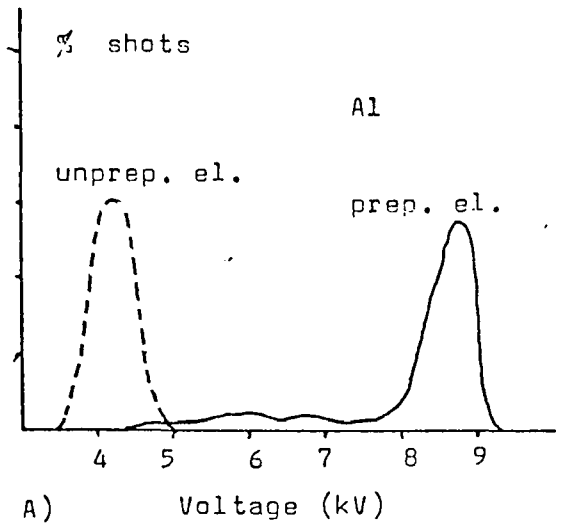

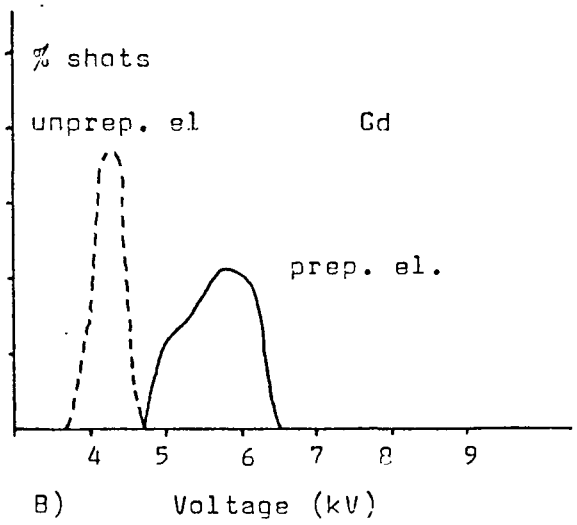

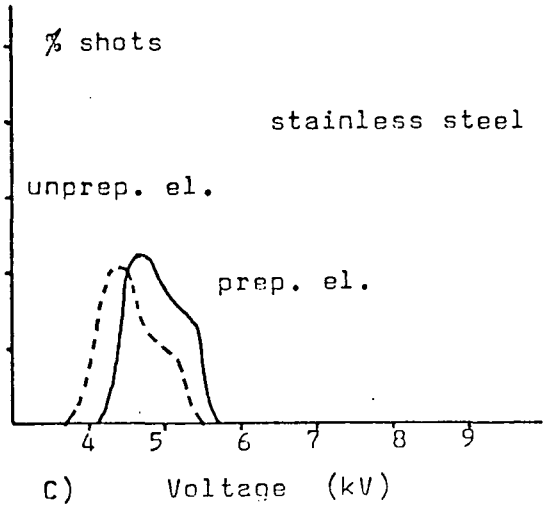

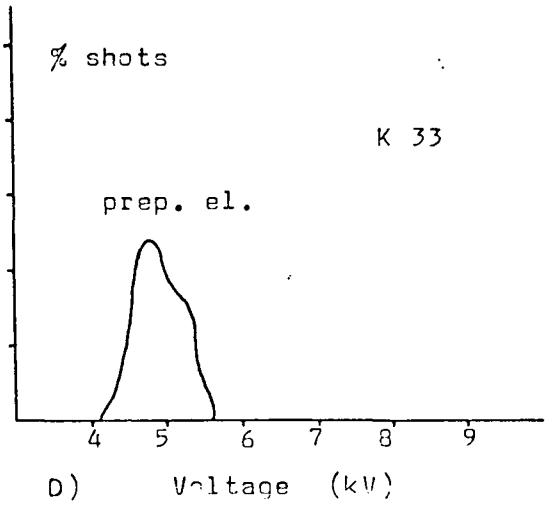

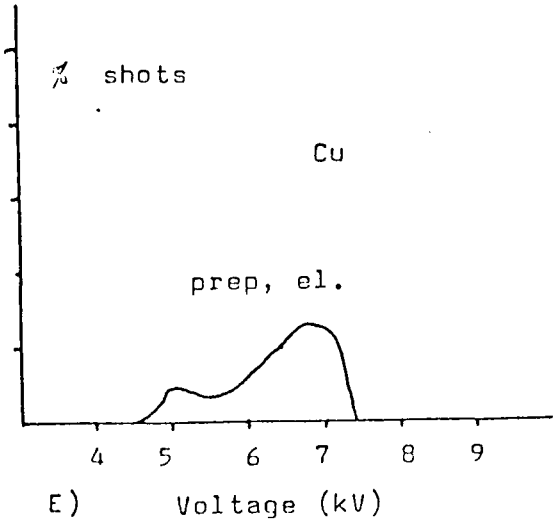

Figs. 2.4.3 Voltage distributions for different electrode material for inductive discharge system.

electrodes than for prepared ones, it is even lower than the breakdown voltage for prepared Gd electrodes. The breakdown voltage for unprepared Gd electrodes is as before somewhat lower.

The steel electrodes are still those which are least dependent on preparation. The difference in breakdown voltage is again within the limits of error.

The voltage distribution for the K33-electrodes is considerably different from the distribution obtained when the capacitive ignition system was used. It could be that the difference is due to the fact that K33 is a composite, and its voltage distribution depends critically on the electrical circuit.

The Cu electrode distribution still has the same characteristic double peak.

We note that when using the inductive ignition system and Al electrodes, there is a possibility of breakdown at low voltages even with prepared electrodes. The voltage distribution looks much like the one obtained with prepared Al electrodes using the capacitive ignition system.

The overall advantage when using the capacitive ignition system is apparently that the voltage distribution is more concentrated in the time scale than it is for the inductive system. The voltage ramp for the capacitive system is approximately 20 times faster than for the inductive system.

2.5.1 Introduction to experiments with capacitively discharged sparks in different gases.

The influence of choice of gas on the breakdown voltage and the voltage distribution were also studied.

According to Meek[4], chapter 6.1.1, the electric field strength at which uniform field breakdown occurs is sometimes called the electric strength of the gas. Inert gases have an electric strength lower than that of other gases. The lower electric strengths of these gases result from the absence of low energy excited states in these gases. In molecular gases an electron looses energy when exciting the molecule to low energy states. Ionization is likely to occur only when the electric field strength is high enough to give an electron the ionization energy within a single free path. In inert gases such energy losses do not occur and the ionization energy may be built up in the course of several elastic collisions. Thus breakdown is achieved relatively easily in the inert gases in spite of their high ionization energies.

2.5.2 Experimental arrangement for sparks in different gases.

In this experiment we used the capacitive discharge circuit (see 2.3.1). A high-voltage probe was used and the voltage ramps were recorded on a digital memory oscilloscope.

The cathode were made of a gold/palladium composite and already mounted on a commercially available sparking plug. This sparking

plug was used in order to minimize the influence of surface condition changes due to chemical reactions.

Five different gases were used: air, oxygen, nitrogen, methan and argon. The sparking plug was mounted in a chamber were pressure could be applied. The sparking plug was discharged 6000 times at a pressure of 1 MPa in the gas used before the measurement was made. The measurements were made at 6 MPa.

2.5.3 Results for different gases.

As expected a lower breakdown voltage is obtained in argon than in other gases; see fig. 2.5.1. We also note that the voltage distribution is somewhat broadened for sparks in nitrogen at 6 MPa compared to the distribution obtained at 1 MPa. The small bumps belong to oxygen (12.5 kV) and nitrogen (14.5 kV). The voltage distribution for air is very close to that of oxygen.

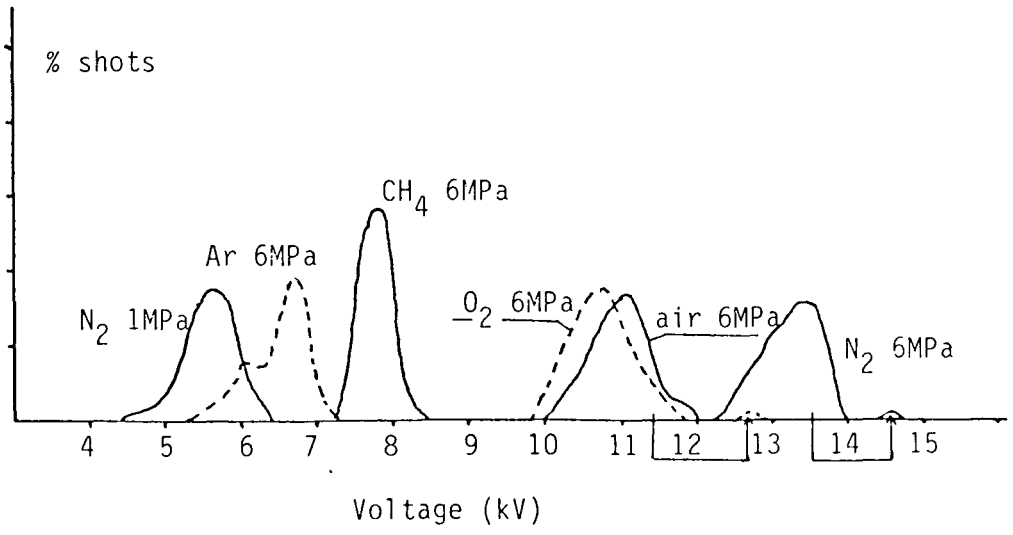

Fig. 2.5.1 : Voltage distributions for sparks in different gases.

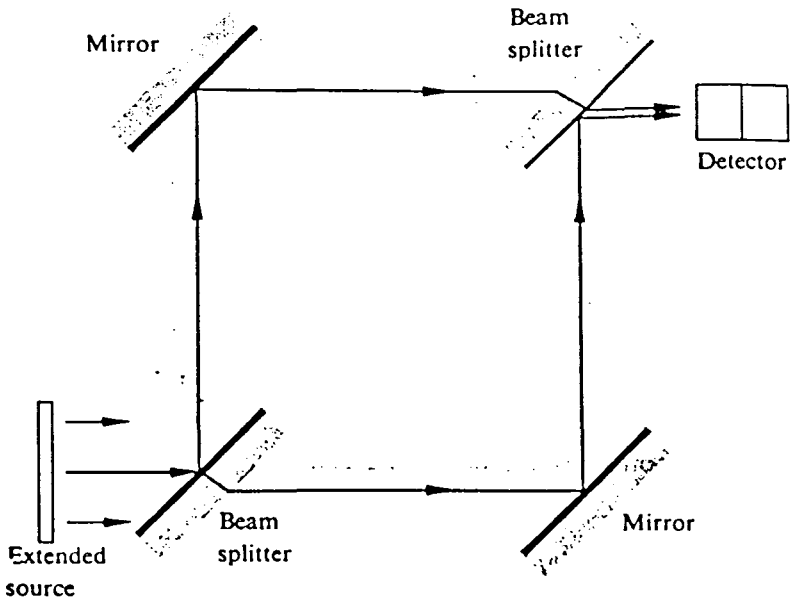

Fig. 3.1.1. Mach-Zender interferometer.

An excimer laser pumped a dye laser, containing the dye Rhodamine 6G. The laser pulse had a wavelength of 590 nm and the energy was 3 mJ in a 15 ns long pulse. The energy was unnecessarily high and a neutral density filter was used to reduce the intensity of the beam to about 20% before allowing it to enter the interferometer. The laser beam was expanded to a diameter of about 4 cm. In the Mach-Zender interferometer the beam is divided into two by a beam splitter and at the exit of the interferometer fringes are obtained due to the difference in optical path between the two beams. A lens at the interferometer exit was focused on the sparking plug and a camera with a 300 mm lens was used to record the events.

A mixture of methane and air was flowed slowly from under the sparking plug; see fig. 3.1.2. After the explosion had taken place

the flame was blown out by pressurized air and the exhaust swept away by a fan.

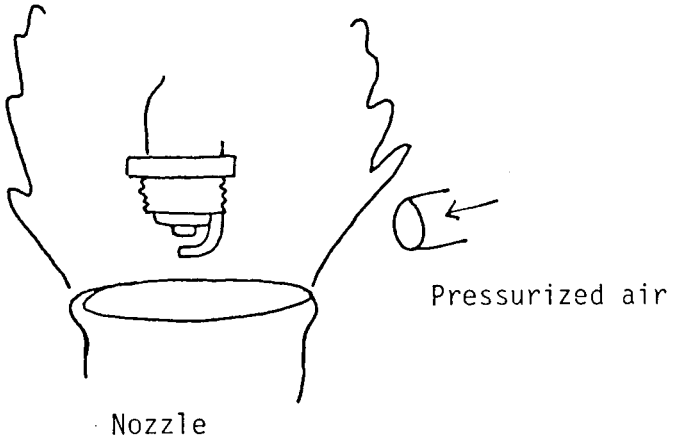

Fig.3.1.2. Sparking plug and nozzle.

A typical flow of gas was 1.9 l/min of air and 0.27 l/min of methan which gives a mixture with 12% methan. The stochiometric value is 9.48%. The area of the circular nozzle was 9.6 cm^2 which means a gas flow of 3.8 cm/s. In 4 ms the gas will flow 0.15 mm and therefore not influence our measurments. When using the inductive ignition system the gas flow for some reason had to be increased in order to ignite the gas. However, the flow is still to slow to influence our mesurments.

The spark was discharged and a delay was used to trig the laser. The time delay from the spark to the laser pulse was easily controlled. The time delay was recorded on an oscilloscope; see fig. 3.1.3. The delay was also used to trig a magnetic valve that released a burst of pressurized air in order to blow out the flame.

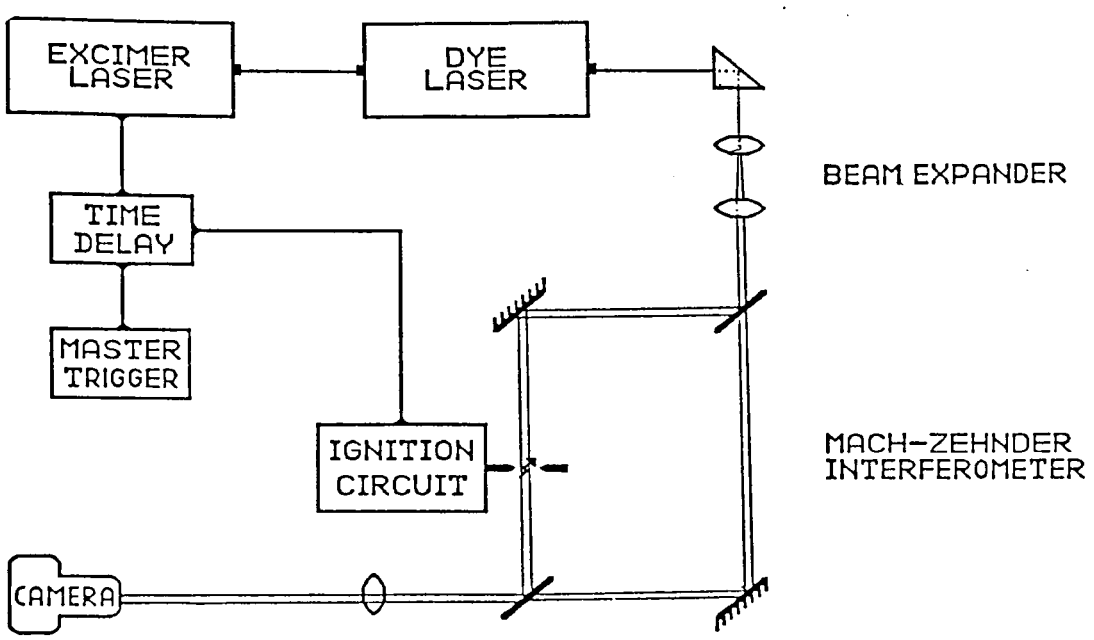

Fig. 3.1.3. Experimental arrangement for time delay measurements.

Typical time delays from the spark to the laser pulse and the recording of the flame front were from 0.1 ms to 4 ms.
The spark was discharged in a conventional sparking plug with steel electrodes (d=0.85 mm) and in a plug where the electrodes had been changed to copper electrodes (d=1.1 mm). In the experiment five photos were taken at each time delay. The time delays were typically 0.1, 1, 2 and 4 ms which makes about 20 photos for each experimental serie. In all, seven series were executed:

1: Inductive ignition, steel electrodes, 9.5% methane. Fig.3.1.4a

2: Inductive ignition, steel electrodes, 11.8% methane.Fig.3.1.4b

3: Inductive ignition, Cu electrodes, 11.1% methane. Fig.3.1.4c

4: Capacitive ignition, steel el, 13.6% methane. Fig.3.1.4d

5: Capacitive ignition, steel el, 12% methane. Fig.3.1.4e

6: Capacitive ignition, Cu electrodes, 13.6% methane. Fig.3.1.4f

7: Capacitive ignition, Cu electrodes, 12% methane. Fig.3.1.4g

3.1.3 Results from flame speed measurments.

In the photos a shadow could often be discerned which indicated the location of the spark on the electrodes. The profile of the sparking plug can be seen in fig. 3.1.5. The location of the spark proved to be of great importance. The sparks which were located on the outer side of the electrodes gave a flame front that was different from the one obtained when the spark was discharged on the inner side of the electrodes, this can be seen in the fringe pattern in fig. 3.1.5B and 3.2.5C.

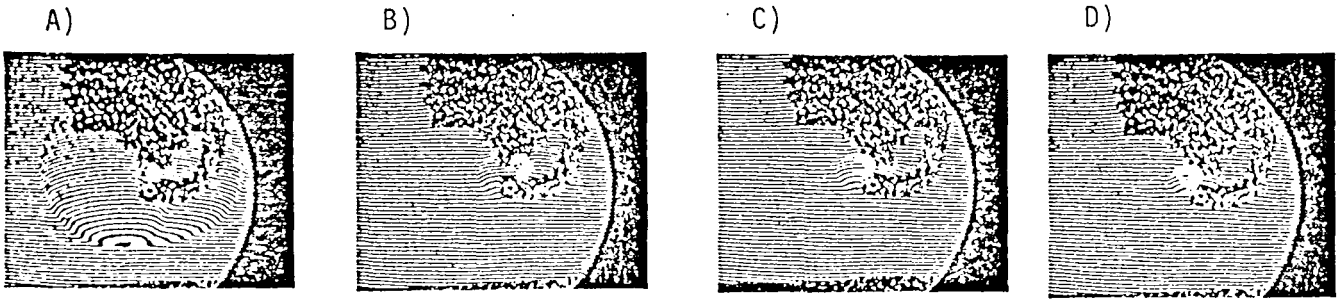

Fig. 3.1.5. Photos at different time delays. A: 4 ms, B: 2 ms, C: 1 ms, D: 0.5 ms.

This means that only discharges in which the sparks were clearly located on the same spot of the electrodes can be compared. In the evaluation the sparks located on the outer region of the electrodes were used.

fig. 3.1.4 Propagation of flamefront as a function of time
a: Inductiv ignition, steel electrodes, 9.5% methane
b: Inductiv ignition, steel electrodes, 11,8% methane
c: Inductiv ignition, Cu electrodes, 11.1% methane

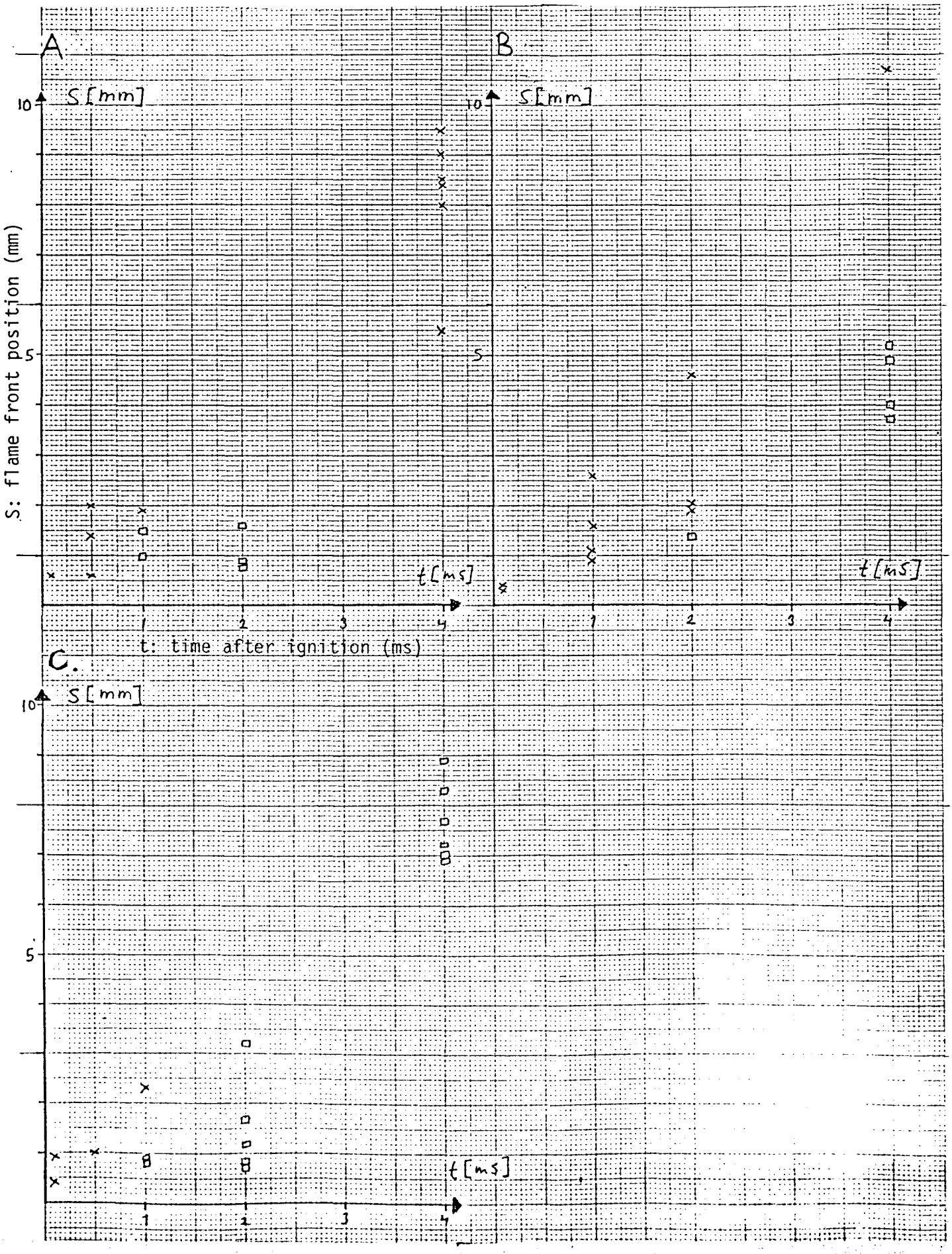

A4 - 1×1 mm

× Combustion clearly originating from outer side of electrode.
□ Other combustion.

fig. 3.1.4 Propagation of flamefront as a function of time.
d: Capacitive ignition, steel electrodes, 13.6% methane
e: Capacitive ignition, steel electrodes, 12% methane
f: Capacitive ignition, Cu electrodes, 13.6% methane
g: Capacitive ignition, Cu electrodes, 12% methane

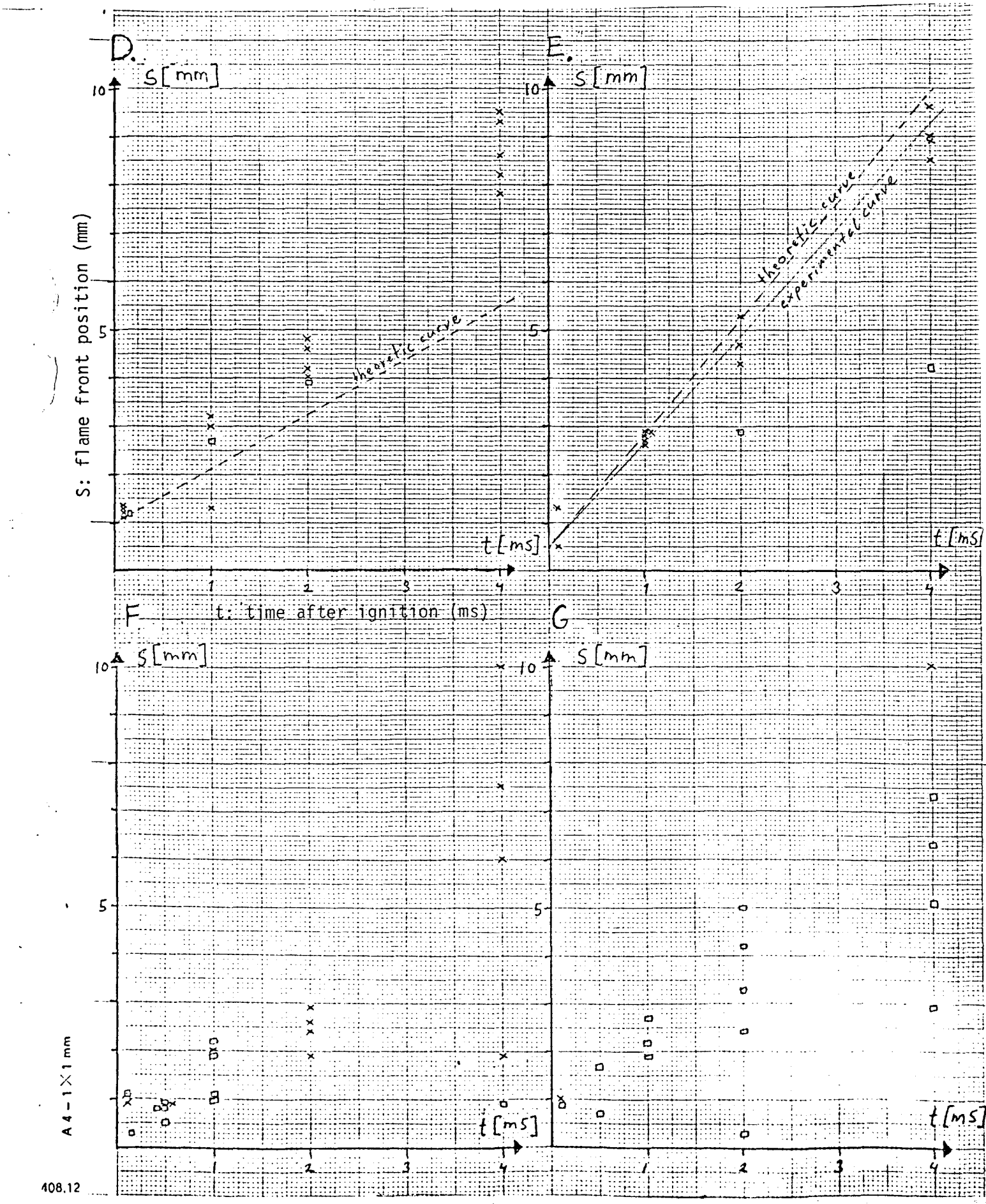

A4 - 1×1 mm

408.12

× Combustion clearly originating from outer side of electrode.

□ Other combustions.

In figs. 3.1.4a-g the results from the series are shown. The flame front is measured from the outer corner of the electrode and straight out horisontally; see fig. 3.1.6.

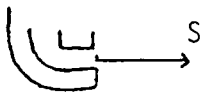

Fig. 3.1.6.

Plotting the propagation of the the flame as a function of time indicated a linear proportionality in some series. For instance, capacitive ignition with steel electrodes and 12% methane gas mixture gave a constant flame speed of 2.3 m/s; see fig. 6.1.4d. Other series, as for instance capacitive ignition with copper electrodes and 13.6% methane gas mixture gave results with such a large spread that they did not admit any curve to be fitted; fig.3.1.4g. All series had in common that for at least one ignition the flame front had propagated 9 mm in 4 ms, what differed was the variance towards slower expansion. In one series, (capacitive ignition, steel electrodes and 13.6% methane gas mixture fig.3.1.4e) the flame front had only propagated 6 mm in 4 ms, in spite of the fact that the spark was located at the outer edge of the electrode.

The flame propagation seems to be almost spherical. A theoretical flame speed can be calculated from the burning velocity of methane-air mixtures, given in ref. 5. The laminar burning velocity is defined as the rate at which a plane combustion wave will propagate into a stationary flammable mixture. This must be distinguished from the flame speed measured in our experiment

since the unburnt gas is here in motion. When the gas in the experiment was burnt it was heated and to maintain atmospherical pressure it had to expand and thereby push away the unburnt gas. The combustion wave can be simplified into the following model, imagine a system boundary around a small volume of gas; see fig. 3.1.7. Let the boundary form a cylinder with a constant cross-section A. Initially all the gas inside the boundary is unburnt and has a temperature T_o and a density d_o. During the combustion the flamefront moves across the system and gas is pushed out through the end area A. Finally all the gas in the system is burnt and has reached a temperature T_f and a density d_f.

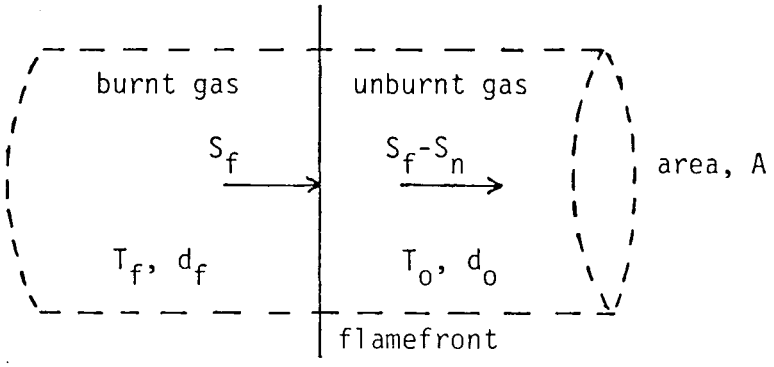

Fig. 3.1.7. Simplified model of combustion.

S_n = laminar burning velocity

S_f = flame front speed (measured in experiment)

T_o = unburnt gas temperature (293 K)

T_f = adiabatic flame temperature

d_o = density of unburnt gas

d_f = density of burnt gas

$S_f - S_n$ = speed at which uncombusted gas is pushed away

A = The area of the invisible boundary where the gas leaves the system

In the calculations below, the influence of the curvature and the thickness of the flame zone is neglected. It is assumed that there is no heat transport and that the combustion does not affect the number of gas molecules. It is also assumed that the general gas law is valid and that the pressure is constant (1 atm) on both sides of the flamefront. The volume of the system is not affected by the combustion and therefore the pV-product is constant through the whole process. The general gas law, pV=nRT, gives that nRT is constant too. Since n is proportional to the density we can write:

$$d_f T_f = d_o T_o \qquad (1)$$

During the propagation of the flamefront through the system unburnt gas is pushed away with a velocity of $S_f - S_n$. This gives:

mass flow leaving system = $(S_f - S_n) d_o A$

This must be equaled by the smaller density in the burnt gas:

decrease of the contense of the system = $S_f(d_o - d_f)A$

These must be identical:

$$(S_f - S_n)d_o = S_f(d_o - d_f) \qquad (2)$$

which gives:

$$S_n d_o = S_f d_f \qquad (3)$$

T_f, the adiabatic flame temperature is the temperature which the gas attains in an adiabatic, isobaric combustion. T_f depends on the pressure, the initial temperature and the initial composition of the system. T_f is calculated by iteration. A value of T_f is

assumed, the atomic conservation equations and equilibrium equations are solved and the final enthalpy is computed and compared with the initial enthalpy. The enthalpy of a mixture as a function of T is calculated from eq. 4 :

$$\sum_i \Delta H_i d_i = \sum_i d_i (\Delta H_{f,i}(T^\circ) + \int_{T^\circ}^{T} C_{p,i}\, dT) \qquad (4)$$

i = index for each species in the mixture.

$\Delta H_{f,i}(T^\circ)$ = creation enthalpy of species i, at standard temperature T° and at standard pressure (1 atm).

$C_{p,i}$ = molar heat capacity of the species i.

d_i = density of species i.

Since the combustion is assumed to be an adiabatic process the enthalpy must be constant. The entire calculation is repeated until a T_f is found which satisfies this condition. These calculations are complicated and are done by computers. The values for T_f and S_n that are used here are calculated by others. T_f for a 10% methan mixture is assumed to be 2223 K (Ref.5), and S_n for a 11.6% methane mixture is 0.33 m/s (Ref.6).

Putting together eqs. 1 and 3 yields, $S_f = (T_f/T_o)S_n =$

$= (2223/293)0.33 = 2.5$ m/s

This result is in accordance with the result from the experiment (using capacitive system, steel electrodes and a 12% methan mixture gives $S_f = 2.3$ m/s experimentally) which indicates that

the combustion is occurring according to the model. However, for a 13.6% methane mixture we obtain S_n=0.17. Assuming the same T_f = 2223 K this gives S_f = 1.3 m/s. This result does not agree well with the experiment; see fig. 3.1.4d.

3.1.4 Conclusions, flame speed measurments.

At atmospheric pressure and a mixture of 12% methane in air and using a capacitive system with steel electrodes a flame speed of 2.3 m/s was measured. But in the remaining six series the variations within the data were too big to allow any curve to be fitted. Therefore it is meaningless to speak about any speed of propagation. The experiment only recorded how far different combustion fronts had travelled after different times. 4 ms after the beginning of the discharge propagations from as low as 1 mm up to 10 mm were measured. These variations were primarily due to the location of the sparks on the electrodes. If a spark was located on the inner sides of the electrodes the combustion was severly delayed. The influence of the ignition system, electrode material and the gas mixture could not be statistically proved. It is quite possible that the variations in the series are due to different time delays between the beginning if the discharge and the ignition of the gas. Here it is impossible to discerne the effects of different time delays from different speeds of propagation. To settle these questions a reproducible spark and a greater statistical material are needed. With a high-speed camera several